Behaviors and high-order harmonic generation for short-range model potential in the intense laser field by using the symplectic algorithm*

LIU Xueshen**, QI Yueying, HUA Wei and DING Peizhu

(Institute of Atomic and Molecular Physics, Jilin University, Changchun 130012, China)

Received October 30, 2003; revised January 7, 2004

Abstract The asymptotic boundary condition to solve the time-dependent Schrödinger equation for a short-range model potential in an intense laser field is presented. The condition is obtained by means of the asymptotic behavior of the short-range model potential in the sufficiently large distance and Fourier transformation, and then the time-dependent Schrödinger equation is discretized into an inhomogeneous linear canonical equation. The inhomogeneous linear canonical equation is solved using the symplectic algorithm. The calculated wavefunctions, time-evolution of the population on the bound state, and the high-order harmonic generation verify that our numerical method is reasonable and effective.

Keywords: asymptotic boundary condition, high-order harmonic generation, symplectic algorithm.

With the devolvement of laser techniques, laser-atom interaction has become one of the very interesting topics[1,2]. In recent years, a number of experiments on intense laser pulses probing laser-atom interaction have produced many new results, such as multiphoton ionization (MPI) rates, above-threshold ionization (ATI) and high-order harmonic generation (HOHG)[3~5]. The high-order harmonics up to order 300 (with the maximum energy about 0.5 keV) have been observed in recent experiments in helium atom[6,7], which has been in the "water windows" range. A lot of theoretical work has been developed in understanding laser-atom interaction, for example, one dimensional binding potential in space has the form $V(x)=-Z/\sqrt{x^2+a^2}$, $-\infty<x<\infty$, where Z is the effective charge and a is a short-range cut-off parameter. This is a quasi-Coulombic or "soft" Coulomb potential. Z and a are introduced to remove the singularity at origin and to adjust the depth of the potential well, and most properties of a real atom can be produced by adjusting the parameters Z and a[8,9]. The ionization rates and harmonic generation for a hydrogen atom were calculated by solving the time-dependent Schrödinger equation[10] and by the state-specific expansion approach[11]. The MPI rates, the spectra of harmonic generation, above-threshold ionization and photoelectron angular distribution were computed from the response of He to strong laser pulses[12,13]. There are many methods[8~13] to numerically solve the time-dependent Schrödinger equation in an intense laser field. Owing to the complexity of an atom in a laser field, the artificial boundary conditions, e.g. an absorber[14] or a mask function[15], are often employed to calculate the time-dependent Schrödinger equation so as to eliminate the reflection of the wavefunction on the boundaries.

As we know, if we do not consider the effect of atomic potential, or the atomic potential is so small that it can be neglected, the atom in a laser field is equivalent to the motion of the electron wavepacket in the laser field. In this paper, we consider the behaviors and high-order harmonic generation for a short-range model potential in the intense laser field. Because the potential is short-range, we neglect the effect of the short-range potential in the sufficiently large distance. Based upon this idea, the asymptotic boundary conditions for solving the time-dependent Schrödinger equation of a short-range model potential in an intense laser field is developed by using Fourier transformation in the sufficiently large distance, and then the time-dependent Schrödinger equation is discretized into an inhomogeneous linear canonical equation by using the asymptotic boundary conditions.

* Supported by the National Natural Science Foundation of China (Grand Nos. 10171039 and 10074019), the Special Funds for Major State Basic Research Projects (Grand No. G1999032804), and the Young Teacher Foundation of Jilin University

** To whom correspondence should be addressed. E-mail: yashuliu@email.jlu.edu.cn

Thus the solutions can be obtained by using the symplectic algorithm.

1 Asymptotic boundary conditions

In the length gauge, the one-dimensional time-dependent Schrödinger equation of the atom in the laser field reads (in atomic units)

$$i\frac{\partial}{\partial t}\psi(x,t)=\left[-\frac{1}{2}\frac{\partial^2}{\partial x^2}+V(x)-\varepsilon(t)x\right]\psi(x,t),$$
$$(t\geqslant 0,\ -\infty<x<+\infty), \tag{1a}$$
$$\psi(x,0)=\varphi(x),\quad \int_{-\infty}^{\infty}|\varphi(x)|^2dx=1,$$
$$(-\infty<x<+\infty), \tag{1b}$$

with the short-range model potential given by

$$V(x)=\frac{-U_0}{\cosh^2(\alpha x)}. \tag{2}$$

This short-range model potential has the following properties:

I. $V(x)=V(-x)$, to ensure that parity is a good quantum number.

II. When $|x|$ is not very big, $|V(x)|$ monotonously decreases.

III. There is a finite number of bound states. If we choose $\alpha=2/(\sqrt{17}-1)$, $U_0=2\alpha^2$ and $S=\frac{1}{2}(\sqrt{1+8U_0/\alpha^2}-1)$, there are two bound states for this short-range potential. The energies are $E_n=-\frac{\alpha^2}{2}(S-n)^2$, $n=0,1$. Thus $E_0=-0.5$, $E_1=-0.0646603$, and the corresponding eigenfunctions are

$$\psi_0=A_0[1-\tanh^2(\alpha x)]^{\frac{\sqrt{-2E_0}}{2\alpha}}, \tag{3}$$

$$\psi_1=A_1\tanh(\alpha x)[1-\tanh^2(\alpha x)]^{\frac{\sqrt{-2E_1}}{2\alpha}}, \tag{4}$$

where A_0 and A_1 are the normalized constant. We add the laser-atom interaction in dipole approximation

$$\varepsilon(t)x=\varepsilon_0 f(t)\cos(\omega_0 t)x. \tag{5}$$

The vector potential $A(t)$ is related to the electric-free amplitude by

$$\varepsilon(t)=-\frac{d}{dt}A(t)=\varepsilon_0 f(t)\cos(\omega_0 t), \tag{6}$$

where ε_0 is the peak intensity of the laser, $f(t)$ is the function that describes the temporal shape of the pulse and the light is assumed to be linearly polarized, and $f(t)=\sin^2(\Omega t)$.

In order to obtain the wavefunction $\psi(x,t)$, we must solve Eq. (1) numerically in the space infinite domain $(-\infty,+\infty)$. However, it is impossible to solve the equation numerically to the infinite boundary, and the computation must be implemented in the finite domain. Thus the difficulty to directly solve the time-dependent Schrödinger equation of a short-range model potential in an intense laser field is to find the proper boundary conditions.

In this section, we concentrate upon the construction of the asymptotic boundary conditions. The initial condition is taken as the ground state eigenfunction, i. e. $\varphi(x)=\psi_0$. Suppose that there is a sufficiently large parameter $X_0>0$. If $|x|\geqslant X_0$, then the potential $V(x)$ and the initial condition $\varphi(x)$ are very small and can be neglected, because the potential $V(x)$ is short-range, which attenuates monotonously with the increase of $|x|$. We omit the effect of the short-range potential in the sufficiently large distance. Eq. (1a) becomes

$$i\frac{\partial}{\partial t}\psi(x,t)=\left[-\frac{1}{2}\frac{\partial^2}{\partial x^2}-\varepsilon(t)x\right]\psi(x,t),$$
$$(t\geqslant 0,\ -\infty<x<+\infty). \tag{7}$$

Eq. (7) and Eq. (1b) can be solved by Fourier transformation. After Fourier transformation, Eq. (7) and Eq. (1b) can be rewritten as:

$$\begin{cases} i\dfrac{\partial\phi(\omega(t),t)}{\partial t}+i\varepsilon(t)\dfrac{\partial\phi(\omega(t),t)}{\partial\omega(t)} \\ \qquad=\dfrac{1}{2}\omega^2\phi(\omega(t),t), \\ \phi(0,\omega(0))=\varphi(\omega(0)). \end{cases} \tag{8}$$

Its solution is

$$\phi(\omega(t),t)=\varphi(\omega(0))\exp\left(-\frac{i}{2}q(t)\right)\cdot\exp(-i\alpha(t)\omega(0))\cdot\exp\left(-\frac{i}{2}\omega^2(0)t\right).$$

After inverse Fourier transformation, we can obtain the solution of Eq. (7)

$$\psi(x,t)=\frac{1-i}{2\sqrt{\pi t}}\exp\left(-iA(t)x-\frac{i}{2}q(t)\right)\cdot\int_{-\infty}^{\infty}\varphi(x')\exp\left(\frac{i(x-\alpha(t)-x')^2}{2t}\right)dx', \tag{9}$$

where $A(t)=-\int_0^t\varepsilon(t')dt'$ is the vector potential, $\alpha(t)=-\int_0^t A(t')dt'$ and $q(t)=\int_0^t A^2(t')dt'$. Eq. (9) is the Volkov function, which expresses an electron wavepacket in a laser field. For $|x|\geqslant X_0$,

$\varphi(x)=0$, then

$$\psi(x,t)=\frac{1-\mathrm{i}}{2\sqrt{\pi t}}\exp\left(-\mathrm{i}Ax-\mathrm{i}\frac{q}{2}\right)\cdot\int_{-X_0}^{+X_0}\varphi(x')\exp\left[\mathrm{i}\frac{(x-\alpha-x')^2}{2t}\right]\mathrm{d}x'.$$

Because $|x|>X_0$ is a sufficiently large real number, when $x'\in[-X_0, X_0]$, the integral function is a rapidly oscillating function. According to the phase integral method[16], we can obtain

$$\int_{-X_0}^{+X_0}\varphi(x')\exp\left[\mathrm{i}\frac{(\pm X-\alpha-x')^2}{2t}\right]\mathrm{d}x'\sim\sqrt{\pi t}(1+\mathrm{i})\varphi(\pm X-\alpha).$$

Thus Eq. (9) can be written as the form at $x=\pm X_0$,

$$\psi(x,t)\mid_{x=\pm X_0}=\exp\left(-\mathrm{i}A(\pm X_0)-\mathrm{i}\frac{q}{2}\right)\cdot\varphi(\pm X_0-\alpha). \tag{10}$$

Let us now consider the behavior of the wavefunction of Eq. (1) on the boundaries. For the short-range potential (2), we can find a sufficiently large parameter $X_0>0$, if $|x|\geqslant X_0$, then $V(x)$ and $\varphi(x)$ are very small. Thus Eq. (10) reflects the asymptotic behavior of the wavefunction of Eq. (1) with the initial wavefunction $\varphi(x)$. That is to say, in the domain $(-\infty, X_0]$ and $[X_0, +\infty)$, the solutions of Eq. (1) are the same as the solutions of Eq. (7) and Eq. (1b). Therefore, on the sufficiently large boundary $x=-X_0$ and $x=X_0$, Eq. (10) can be used as the boundary conditions of Eq. (1). We call Eq. (10) the asymptotic boundary conditions. Thus Eq. (1) can be solved numerically in the finite domain $[-X_0, X_0]$ by using the asymptotic boundary conditions (10).

Note that if the initial wavefunction $\varphi(x)$ is normalized, the wavefunction $\psi(x,t)$ is also normalized $\int_{-\infty}^{+\infty}|\psi(x,t)|^2\mathrm{d}x=1$. Therefore, the norm of the wavefunction inside the boundaries is given by

$$N=\int_{-X_0}^{+X_0}|\psi(x,t)|^2\mathrm{d}x=1-\int_{-\infty}^{-X_0}|\psi(x,t)|^2\mathrm{d}x-\int_{+X_0}^{+\infty}|\psi(x,t)|^2\mathrm{d}x\leqslant 1. \tag{11}$$

Eq. (11) results from the electron wavepacket moving outside the boundary. In the computation the boundary is much larger than the maximum radius of the quiver motion of the electron, the probability of the electron outside the boundaries is very small, and the electron that has gone outside the boundaries is regarded as ionization[14]. Thus we ignore the contributions of the wavefunction outside the boundaries in the following computation. This is a good approximation in case that the boundaries are properly large.

2 Numerical recipe

The fundamental theorem of Hamiltonian mechanics says that the time-evolution of the Hamiltonian system is the evolution of symplectic transformation. In this sense, we say that the Hamiltonian system has a symplectic structure. Therefore, Ruth[17] and Feng[18] presented the symplectic algorithm for solving the Hamiltonian system, and found a new method for solving the Hamiltonian system.

Symplectic algorithm is a difference method that preserves the symplectic structure, and is a better method in the long-time many-step calculation and can preserve the structure of the system.

At present, the study and application of symplectic algorithm has been developed[19~25]. For example, symplectic algorithm is used to calculate the water wave equation, Kdv equation, Schrödinger equation, Celestial mechanics equation and so on.

We have presented the symplectic scheme-matrix eigenvalue method and the symplectic scheme-shooting method for solving the time-independent Schrödinger equation recently[26~28], and demonstrated that our numerical method is stable and effective for solving the eigenvalue of the time-independent Schrödinger equation.

We can also use the symplectic algorithm to solve Eq. (1) with the boundary conditions (10). Let $\psi(x,t)=q(x,t)+\mathrm{i}p(x,t)$, $U(x,t)=V(x)-\varepsilon(t)x$. Suppose N is a sufficiently large positive integer, the whole space $(-X_0, +X_0)$ can be divided into $2N$ equal segments, and the length of each segment is $h=X_0/N$. Denoting $x_j=jh$, $j=-N, -N+1, \cdots, -1, 0, 1, \cdots, N-1, N$, such that boundary conditions (10) can be written as:

$$\begin{cases}\psi(t,-X_0)=q_{-N}+\mathrm{i}p_{-N},\\ \psi(t,+X_0)=q_N+\mathrm{i}p_N.\end{cases} \tag{12}$$

Substituting the symmetry difference quotient for the partial derivative, we have $\frac{\partial^2\psi}{\partial x^2}=\frac{\psi_{-1}-2\psi+\psi_{+1}}{h^2}$.

Eq. (1) can be discretized into the following $(2N-1)$-dimensional Hamiltonian inhomogeneous linear canonical equation[29]

$$\begin{cases} \dot{P} = -SQ + Y_2, \\ \dot{Q} = SP - Y_1, \end{cases} \tag{13}$$

where $P=(p_{-N+1}, \cdots, p_{-1}, p_0, p_1, \cdots, p_{N-1})^{\mathrm{T}}$, $Q=(q_{-N+1}, \cdots, q_{-1}, q_0, q_1, \cdots, q_{N-1})^{\mathrm{T}}$, $Y_1 = \frac{1}{2h^2}(p_{-N}, 0, \cdots, 0, p_N)^{\mathrm{T}}$, $Y_2=\frac{1}{2h^2}(q_{-N}, 0, \cdots, 0, q_N)^{\mathrm{T}}$ and "T" denotes the transposed matrix, $\boldsymbol{S}$ is a symmetry matrix

$$\boldsymbol{S}=\begin{bmatrix} U_{-N+1}+\frac{1}{h^2} & -\frac{1}{2h^2} & 0 & 0 & \cdots & 0 \\ -\frac{1}{2h^2} & U_{-N+2}+\frac{1}{h^2} & -\frac{1}{2h^2} & 0 & \cdots & 0 \\ 0 & \ddots & \ddots & \ddots & & \vdots \\ \vdots & & \ddots & \ddots & \ddots & 0 \\ 0 & \cdots & 0 & -\frac{1}{2h^2} & U_{N-2}+\frac{1}{h^2} & -\frac{1}{2h^2} \\ 0 & \cdots & 0 & 0 & -\frac{1}{2h^2} & U_{N-1}+\frac{1}{h^2} \end{bmatrix}.$$

If we let $Z=(P^{\mathrm{T}}, Q^{\mathrm{T}})^{\mathrm{T}}$, $Y=(Y_1^{\mathrm{T}}, Y_2^{\mathrm{T}})^{\mathrm{T}}$, then inhomogeneous linear canonical equation can be written as the form

$$\frac{\mathrm{d}Z}{\mathrm{d}t} = GZ - J^{-1}Y = J^{-1}CZ - J^{-1}Y, \tag{14}$$

where $G=\begin{bmatrix} 0 & -S \\ S & 0 \end{bmatrix} = J^{-1}C$, $J=\begin{bmatrix} 0 & I \\ -I & 0 \end{bmatrix}$, $C=\begin{bmatrix} S & 0 \\ 0 & S \end{bmatrix}$. The solutions of Eq. (14) are

$$Z(t) = g_G^{0,t}Z_0 - \int_0^t g_G^{\tau,t} J^{-1} Y(\tau)\mathrm{d}\tau. \tag{15}$$

In particular, the time-evolution from one time to another is

$$Z^{k+1} = g_G^{t_k, t_{k+1}} Z^k - \int_{t_k}^{t_{k+1}} g_G^{\tau, t_{k+1}} J^{-1} Y(\tau)\mathrm{d}\tau, \tag{16}$$

where $g_G^{\tau,t} = \exp\left(\int_r^t G(t)\mathrm{d}t\right)$ is a symplectic transformation. We have recently presented the symplectic algorithm for solving the inhomogeneous linear canonical equation (14), and in Ref. [29] we give a two-order symplectic scheme for solving the inhomogeneous linear canonical equation (14). From Eq. (16), we can know that the normalization of the system is conservative if there is no inhomogeneous term $J^{-1}Y$. Thus, the term of $\int_{t_k}^{t_{k+1}} g_G^{\tau,t_{k+1}} J^{-1} Y(\tau)\mathrm{d}\tau$ expresses the escape of the electron wavefunction to the outside boundaries from t_k to t_{k+1}.

3 Results and discussions

To investigate the behavior and high-order harmonic generation of the laser-atom interaction for short-range potential (2) in the intense laser field by using the asymptotic boundary conditions (10) and the symplectic algorithm, we select the short laser pulses of wavelength 828 nm ($\omega=0.055$ a.u.) and intensities in the range of $1.7\times10^{15} \sim 7.00\times10^{15}$ W/cm^2 ($\varepsilon_0=0.05 \sim \varepsilon_0=0.20$ a.u.). The electric field profile of the laser is taken as the square of sine with 5 light periods. The initial state $\varphi(x)$ is taken as the wavefunction (3) of the ground state.

3.1 Evolution of the norm of the wavefunction inside the boundaries with time

To illustrate the numerical method, we first compute the evolution of the norm of the wavefunction inside the boundaries with time. From Eq. (11), one knows that the motion outside the boundaries makes the norm of the wavefunction inside the boundaries less than or equal to 1. In the computation, we choose $X_0=1000$ a.u. The evolution of the norm of the wavefunction inside the boundaries with time is shown in Fig. 1. Fig. 1(a) shows the norm of the wavefunction for intensity $\varepsilon_0=0.05$ a.u. The norm of the wavefunction is preserved to be 10^{-7}, because the intensity is very small and most electrons move inside the boundaries. Fig. 1(b) shows the norm of the wavefunction for intensity $\varepsilon_0=0.14$ a.u. However, the norm of the wavefunction inside the boundaries is only a little smaller than 1 after the maximum of the laser field, which indicates that the probability of the electron outside the boundaries is very small and thus the calculation with the function inside the boundaries is convergent.

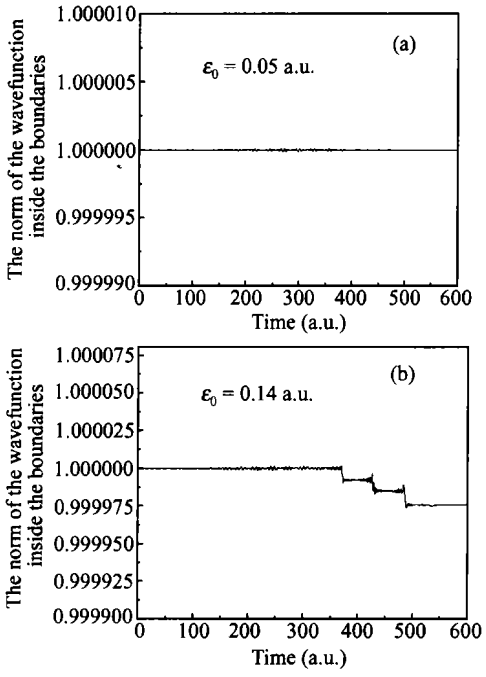

Fig. 1. Evolution of the norm of the wavefunction inside the boundaries with time. (a) $\varepsilon_0 = 0.05$ a.u.; (b) $\varepsilon_0 = 0.14$ a.u.

3.2 The behavior of the wavefunction

To verify the numerical method, we also compare the behavior of the wavefunction computed using different boundary parameter X_0. Fig. 2 shows the spatial distributions of the wavefunction at $t = 500$ a.u.

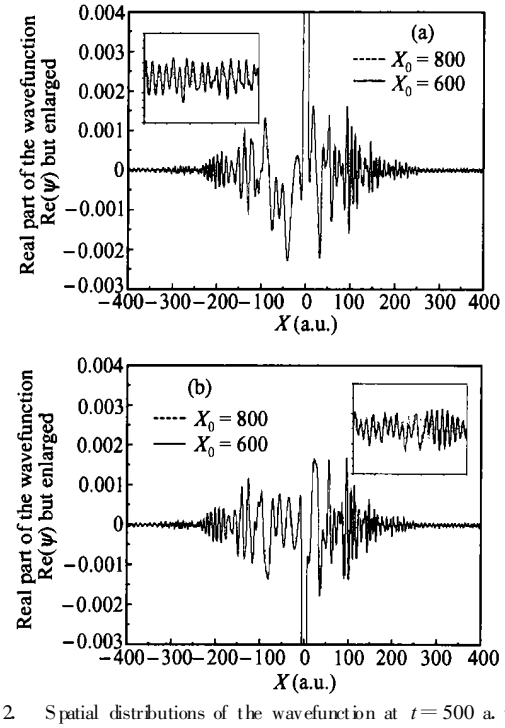

Fig. 2. Spatial distributions of the wavefunction at $t = 500$ a.u., $\varepsilon_0 = 0.05$ a.u. (a) The real part of the wavefunction, (the inset shows the result from -600 to -500); (b) the imaginary part of the wavefunction (the inset shows the result from 500 to 600).

and the peak intensity of the laser $\varepsilon_0 = 0.05$ a.u. Two calculations with the boundaries of $X_0 = 600$ a.u. and $X_0 = 800$ a.u. are carried out. The dot line is calculated in the range of $[-800, 800]$ and the solid line is calculated in the range of $[-600, 600]$. The two calculations yield results that are almost not distinguishable inside the boundaries. The insets show the wavefunctions near the boundaries. It can be seen from the figures that the solid line and the dot line are almost the same, which verifies that our numerical method is reasonable and effective.

3.3 Probability density $|\psi|^2$ (or modulus squared) of the wavefunction

The numerical wavefunction may be the characteristic of the above-threshold-ionization peak. Plots of the probability density will usually reveal this process. Fig. 3 shows the probability density $|\psi|^2$ versus X at $t = 500$ a.u. for different laser peak intensity. The plateau regions are about $(-350, 350)$, $(-450, 450)$, $(-700, 700)$ and $(-900, 900)$ for the laser peak intensity of $\varepsilon_0 = 0.08$ a.u., $\varepsilon_0 = 0.12$ a.u., $\varepsilon_0 = 0.16$ a.u., and $\varepsilon_0 = 0.20$ a.u., respectively. The higher the laser intensity is, the wider the plateau region is. Since electron emission continuously takes place over the duration of the calculation, for higher laser intensity, the probability densities can extent to far distance.

3.4 Time evolution of the population on the ground state (the initial state) and the bound state

The total time-dependent ionization population can be calculated by the formula:

$$P_{\text{ion}}(t) = \int |\langle \psi_k(x) \Psi(x, t)\rangle|^2 dk = 1 - \sum_{\text{bound}} |\langle \psi_n(x) | \Psi(x, t)\rangle|^2,$$

where $\psi_k(x)$ is any state of the continuum, $\psi_n(x)$ is the wavefunction of the bound state. The summation is over all the bound state $\psi_n(x)$ when the field has been turned off. Thus the population of the bound state is

$$P_{\text{bound}}(t) = \sum_{\text{bound}} |\langle \psi_n(x) | \Psi(x, t)\rangle|^2.$$

Because there are only two bound states for the short-range potential, the population on the ground state (the initial state) and all bound states are

$$P_{\text{1b}}(t) = |\langle \psi_0(x) | \Psi(x, t)\rangle|^2,$$

$$P_{\text{b}}(t) = |\langle \psi_0(x) | \Psi(x, t)\rangle|^2 + |\langle \psi_1(x) | \Psi(x, t)\rangle|^2.$$

In the computation, we choose $X_0 = 1000$ a.u., and the time evolution of the population on the ground state and all bound states with time are shown in Fig. 4 for short-range potential in the laser field with different peak intensity of the laser. In Fig. 4, the dot line is the population of all bound states (i.e. the ground state and the first excited state) and the solid line is the population of the ground state. It can be

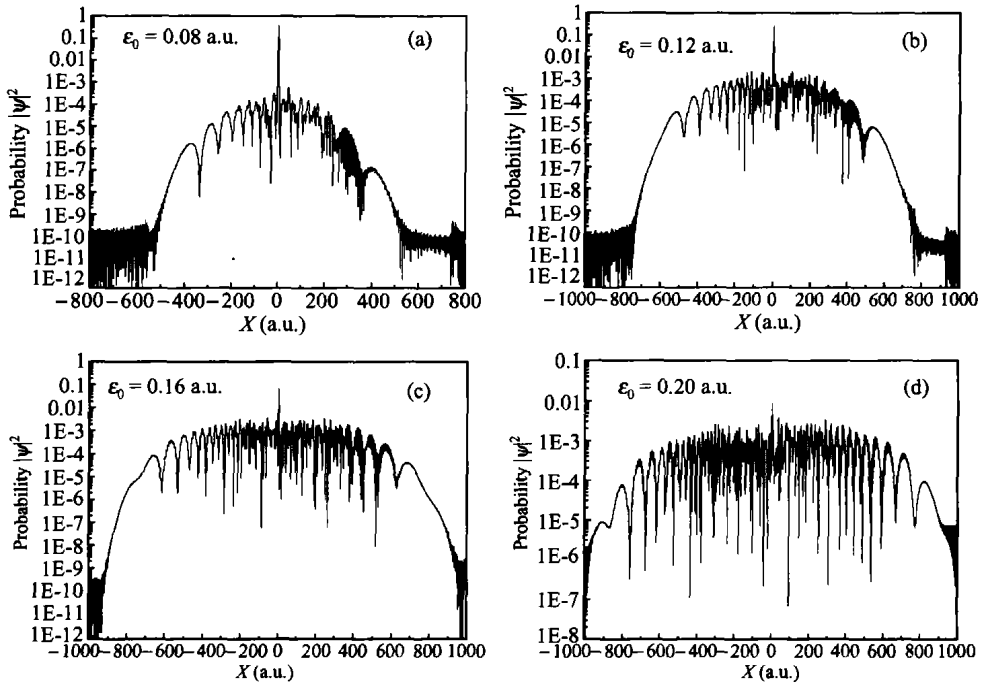

Fig. 3. Probability density $|\psi|^2$ (or modulus squared of the wavefunction) vs X at $t = 500$ a.u. (a) $\varepsilon_0 = 0.08$ a.u.; (b) $\varepsilon_0 = 0.12$ a.u.; (c) $\varepsilon_0 = 0.16$ a.u.; (d) $\varepsilon_0 = 0.20$ a.u.

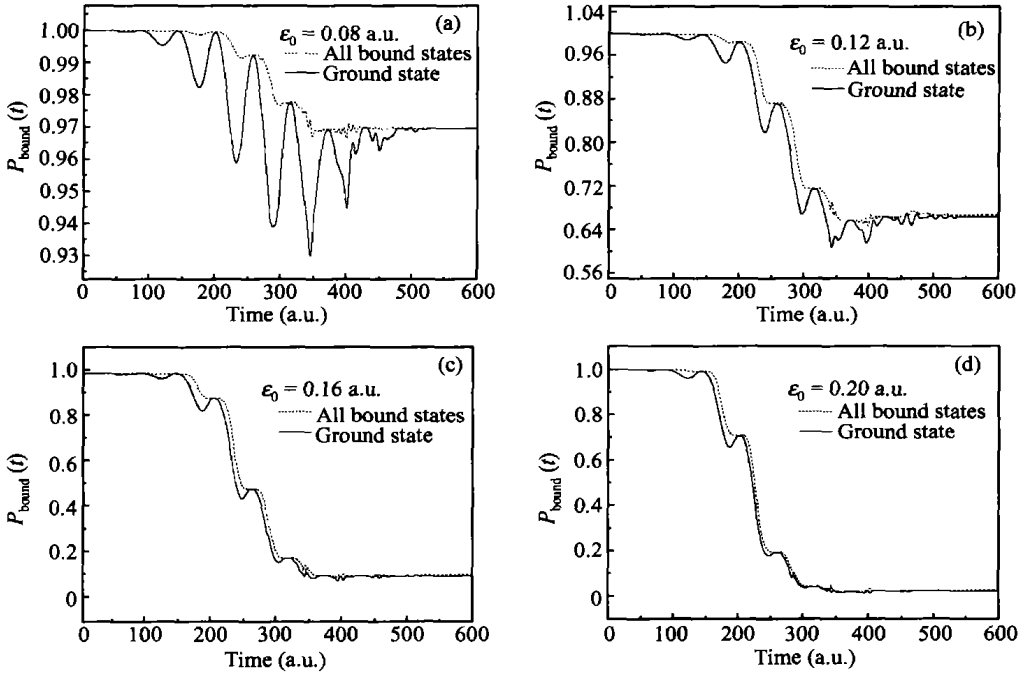

Fig. 4. Time evolution of the population on the ground state and all bound states. (a) $\varepsilon_0 = 0.08$ a.u.; (b) $\varepsilon_0 = 0.12$ a.u.; (c) $\varepsilon_0 = 0.16$ a.u.; (d) $\varepsilon_0 = 0.20$ a.u.

seen from Fig. 4 that the higher the laser peak intensity is, the smaller the minimum probability on the bound state is, which reveals that the population on the bound state decreases with the increase of the laser peak intensity. For low laser peak intensity, most of the population is in the bound state, especially for $\varepsilon_0=0.08$ a.u., it is very clear that the ground state population is more than 0.93 and oscillates. However, with the increase of the laser peak intensity, the bound state population becomes smaller and smaller. For $\varepsilon_0=0.20$ a.u. and $t=300$ a.u., the bound state population is almost zero. This means that most of the population is in the state of the continuum for higher laser peak intensity.

3.5 High-order harmonic generation

We also investigate high-order harmonic of the short-range potential in the laser field. The dipole acceleration is given by

$$d(t)=-\int_{-X_0}^{X_0}\psi^*(x,t)\frac{\partial V}{\partial x}\psi(x,t)\mathrm{d}x+E(t).$$

The Fourier transformation of $d(t)$ is calculated by

$$d(\omega)=\frac{1}{T_2-T_1}\frac{1}{\omega^2}\int_{T_1}^{T_2}d(t)\mathrm{e}^{-\mathrm{i}\omega t}\mathrm{d}t.$$

The intensity of the high-order harmonic spectrum is proportional to $|d(\omega)|^2$. In the computation, we choose $X_0=1000$ a.u. Fig. 5 displays the high-order harmonic spectrum of short-range potential in the laser field with different peak intensity of the laser, the distribution of the harmonic spectrum exhibits the same characteristic behavior, i.e. a rapid decrease for the first few low-order harmonics, then a plateau where all the harmonics have nearly the same strength, and finally a rather sharp cut-off. The order of cut-off is in agreement with the predicted formula $I_p+3.2U_p$, where I_p is the ionization potential, $U_p=\frac{\varepsilon_0^2}{4\omega_0^2}$ is the ponderomotive energy of the electron quivering in the laser field with the amplitude of the electron field ε_0 and the laser frequency ω_0.

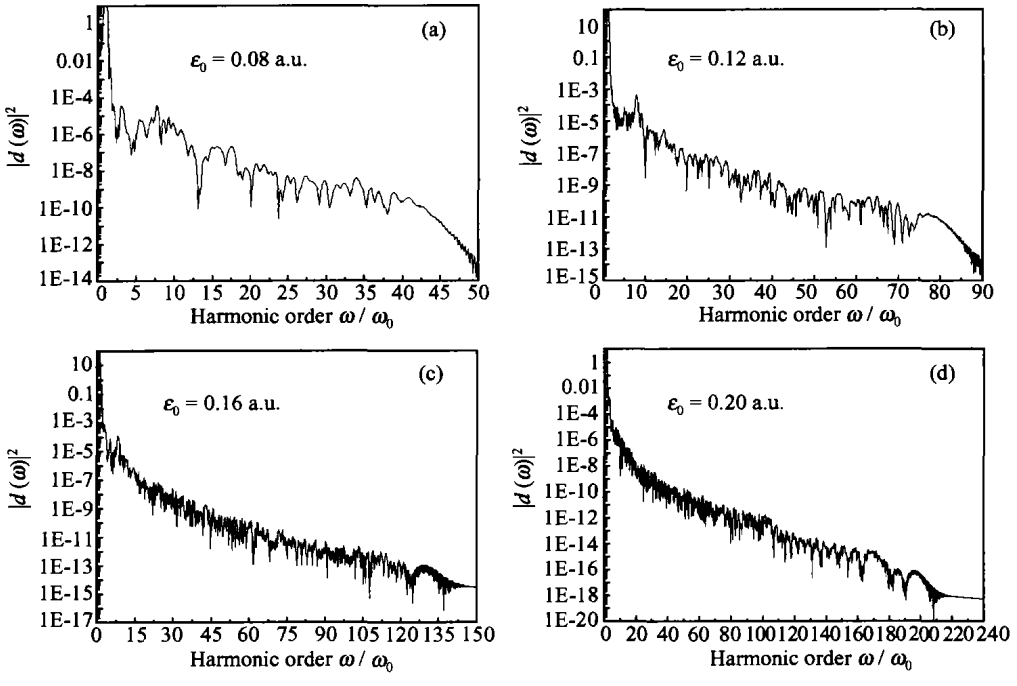

Fig. 5. High-order harmonic generation. (a) $\varepsilon_0=0.08$ a.u.; (b) $\varepsilon_0=0.12$ a.u.; (c) $\varepsilon_0=0.16$ a.u.; (d) $\varepsilon_0=0.20$ a.u.

(i) $\varepsilon_0=0.08$ a.u. (2.8×10^{15} W/cm^2)

We can see from Fig. 5(a) that there is a cut-off at the 40th harmonic ($I_p+3.2U_p=40\omega_0$). The harmonic strength is nearly 10^{-8} and the plateau is very distinct.

(ii) $\varepsilon_0=0.12$ a.u. (4.2×10^{15} W/cm^2)

In Fig. 5(b), the cut-off for the laser peak intensity $\varepsilon_0=0.12$ a.u. is around 78th, which is in good agreement with the predicted formula $I_p+3.2U_p$. The plateau is also distinct but there is a lit-

tle decrease.

(iii) $\varepsilon_0 = 0.16$ a.u. (5.6×10^{15} W/cm^2)

There is a cut-off at the 132nd which is still in agreement with the formula $I_p + 3.2U_p$ for the laser peak intensity $\varepsilon_0 = 0.16$ a.u. in Fig. 5(c), but the plateau is not distinct and there is a little decline.

(iv) $\varepsilon_0 = 0.20$ a.u. (7.0×10^{15} W/cm^2)

There is an abrupt decrease at the 109th harmonic and an extended lower intensity plateau reaching the 201st harmonic ($I_p + 3.2U_p = 201\omega_0$) in Fig. 5(d). It is still in agreement with the formula $I_p + 3.2U_p$. If the laser peak intensity increases, the cut-off is at around the abrupt harmonic and there is no extended lower intensity plateau. Meanwhile, the order of cut-off is not in agreement with the formula $I_p + 3.2U_p$. We think that these harmonic characteristics indicate that the laser peak intensity reaches the saturation intensity. For this system the saturation intensity is around 0.20 a.u.

In summary, we have presented the asymptotic boundary conditions for solving the time-dependent Schrödinger equation of a short-range model potential in an intense laser field. The time-dependent Schrödinger equation is discretized into the inhomogeneous linear canonical equations and is computed by using the symplectic algorithm. The behavior and high-order harmonic generation of the laser-atom interaction for short-range potential in the intense laser field by using the asymptotic boundary conditions and the symplectic algorithm are investigated, we choose the short laser pulses of wavelength 828 nm ($\omega = 0.055$ a.u.) and intensities in the range of $1.7\times10^{15} \sim 7.00\times10^{15}$ W/cm^2 ($\varepsilon_0 = 0.05 \sim \varepsilon_0 = 0.20$ a.u.). The electric field profile of the laser is taken as the square of sine with 5 light periods. We compute the evolution of the norm of the wavefunction inside the boundaries with time and the behavior of the wavefunction for different calculations with the boundaries $X_0 = 600$ a.u. and $X_0 = 800$ a.u. The norm of the wavefunction inside the boundaries is less than or equal to 1, the spatial distributions of the wavefunction is the same for different calculations with different boundaries. These results have verified that our numerical method is reasonable and effective. Probability density of the wavefunction and the time evolution of the population on bound state are calculated. We also study high-order harmonic generation of short-range potential in the laser field for different laser peak intensity; the order of cut-off is in agreement with the predicted formula $I_p + 3.2U_p$. The saturation intensity is thought to be around 0.20 a.u. for this system.

Acknowledgment The authors would like to thank Professor Zhou Z. Y. and Dr. Liu X. Y. for their helpful discussions and suggestions.

References

1 Eberly, J. H. et al. High-order harmonic production in multiphoton ionization. J. Opt. Soc. Am. B, 1989, 6(7): 1289.
2 Sanpera, A. et al. Resonant and nonresonant effects in the multiphoton detachment of a one-dimensional model ion with a short-range potential. J. Opt. Soc. Am. B, 1991, 8(8): 1568.
3 L'Huillier, A. et al. High-order harmonic generation in rare gases with a 1-ps 1053-nm laser. Phys. Rev. Lett., 1993, 70(6): 774.
4 Macklin, J. J. et al. High-order harmonic generation using intense femtosecond pulses. Phys. Rev. Lett., 1993, 70(6): 766.
5 Shin, H. J. et al. Generation of nonadiabatic blueshift of high harmonics in an intense femtosecond laser field. Phys. Rev. Lett., 1999, 83(13): 2544.
6 Schurer, M. et al. Coherent 0.5-keV X-Ray Emission from Helium Driven by a Sub-10-fs Laser. Phys. Rev. Lett., 1998, 80: 3236.
7 Chang, Z. H. et al. Generation of coherent soft X rays at 2.7 nm using high harmonics. Phys. Rev. Lett., 1997, 79: 2967.
8 Liu, W. C. et al. Closed-form solutions of the Schrödinger equation for a model one-dimensional hydrogen atom. J. Phys. B: At. Mol. Opt. Phys., 1992, 25: L517.
9 Su, Q. et al. Model atom for multiphoton physics. Phys. Rev. A, 1991, 44: 5997.
10 LaGattuta, K. J. Two-photon ionization rates of atomic hydrogen: comparison of numerical and analytical techniques. J. Opt. Soc. Am. B, 1993, 10(5): 958.
11 Dionissopoulou, S. et al. Ionization rates and harmonic generation for H interacting with laser pulses of $\lambda = 1064$ nm and peak intensities in the range $2\times10^{13} \sim 2\times10^{14}$ W·cm^{-2}. J. Phys. B: At. Mol. Opt. Phys., 1996, 29: 4787.
12 Nicolaides, C. A. et al. The significance of electron correlation and of state symmetries in the interaction of strong laser pulses of 5 eV with He. J. Phys. B: At. Mol. Opt. Phys., 1998, 31: L1.
13 Mercouris, T. et al. Multiphoton response of He to short laser pulses of wavelength 248 nm and intensities in the range $10 \sim 10$ W·cm^{-2}. J. Phys. B: At. Mol. Opt. Phys., 1997, 30: 4751.
14 Lappas, D. G. et al. Generation of attosecond xuv pulses in strong laser-atom interactions. Phys. Rev. A, 1998, 58: 4140.
15 Hu, S. X. et al. Dynamics of an intense laser-driven multi well system: A model of ionized clusters. Phys. Rev. A, 1997, 56: 3916.
16 Heading, J. An Introduction to Phase Integral Methods. London: Methuen and Co., 1962.
17 Ruth, R. D. A canonical integration technique. IEEE Trans. Nuc. Sci., 1983, 30: 2669.
18 Feng, K. Difference schemes for Hamiltonian formalism and symplectic geometry. J. Comput. Math., 1986, 4: 279.
19 Leimkuhler, B. J. et al. Symplectic numerical integrators in constrained Hamiltonian system. J. Comput. Phys., 1994, 112: 117.

20 Yoshida, H. Construction of higher order symplectic integrators. Phys. Lett. A, 1990, 150: 262.
21 Ding, P. Z. et al. Square-preserving and symplectic structure and scheme for quantum system. Chin. Phys. Lett., 1996, 13: 245.
22 Zhu, W. S. et al. Numerical methods with a high order of accuracy applied in the quantum system. J. Chem. Phys., 1996, 104 (6): 2275.
23 Gray, S. K. et al. Classical Hamiltonian structures in wave packet dynamics. J. Chem. Phys., 1994, 100(7): 5011.
24 Gray, S. K. et al. Symplectic integrators tailored to the time-dependent Schrödinger equation. J. Chem. Phys., 1996, 104(18): 7099.
25 Zhou, Z. Y. et al. Study of a symplectic scheme for the time evolution of an atom in an external field. J. Korean Phys. Soc., 1998, 32: 417.
26 Liu, X. S. et al. Numerical solution of one-dimensional time-independent Schrödinger equation by using symplectic schemes. Intern. J. Quantum Chem., 2000, 79(6): 343.
27 Liu, X. S. et al. Numerical solution of a two-dimensional time-independent Schrödinger equation by using symplectic schemes. Intern. J. Quantum Chem., 2001, 83(5): 303.
28 Liu, X. S. et al. Symplectic algorithm for use in computing the time-independent Schrödinger equation. Intern. J. Quantum Chem., 2002, 87(1): 1.
29 Liu, X. Y. et al. The symplectic method for solving the linear inhomogeneous canonical equations in 1-dimensional intense field model. Chin. J. Comput. Phys., 2002, 19: 60.